ROYAL SOCIETY OF CHEMISTRY

PAPER

Check for updates

Eco design for Ag-based solutions against SARS-CoV-2 and *E. coli*†

Anna Luisa Costa, [iD] *[a] Magda Blosi, [iD] *[a] Andrea Brigliadori, [iD] [a] Ilaria Zanoni,[a] Simona Ortelli, [iD] [a] Felice Carlo Simeone, [iD] [a] Serena Delbue,[b] Sarah D'Alessandro,[c] Silvia Parapini,[d] Claudia Vineis,[e] Alessio Varesano, [iD] [e] Muhammet S. Toprak, [iD] [f] Bejan Hamawandi[f] and Davide Gardini[a]

For the first time, we exploited the antiviral and antibacterial properties of Ag NPs stabilised by quaternized hydroxyethyl cellulose (Ag-HEC) against SARS-CoV-2 and *Escherichia coli* through an eco-friendly process at room temperature in three different environments: 1) water, where Ag was dispersed as a nanosol, 2) textiles, where Ag was applied as a coating, and 3) hydrogel where Ag is embedded. The antiviral performance of Ag-HEC nanosols was quantified through the selectivity index (SI), defined as the ratio between 50% cytotoxic and inhibitory concentration, in order to evaluate the ability to be active in a concentration range below the cytotoxicity value. The collected results pointed out an actual enhanced risk/benefit profile of Ag-HEC NPs with respect to chloroquine, with an SI of 22.2 and 8.4, respectively. Antibacterial and antiviral activities of Ag-HEC NPs immobilized on textiles or mucosa-like hydrogels were also assessed and their efficacy in potential application as protective clothing or nasal molecular masks was verified. This work demonstrated that a modern, safe and sustainable design allows traditional colloidal silver-based technologies to be efficiently exploited for a broad spectrum of antimicrobial solutions against bacterial and viral infections.

Environmental significance

Antimicrobial nano silver-based solutions have been investigated since ancient times, but more than ever need reliable and sound strategies for their eco design and verification. Our easily scalable synthetic route, transforming benign reagents, at room temperature, with almost complete yield, matches sustainability criteria. The produced AgHEC nanosol tested against SARS-CoV 2 overcomes the big safety challenge of improving selectivity and identifying use conditions where the antimicrobial activity is maximum, and toxicity is below the identified threshold limits (selectivity index > 10). The reduction, or suppression, of bacterial and viral activities of AgHEC, also verified in textile coatings or hydrogel matrices, supports the use of Ag-HEC as an effective antimicrobial agent for the industrial production of protective clothing or nasal molecular masks.

1. Introduction

[a] *National Research Council of Italy, Institute of Science and Technology for Ceramics (CNR-ISTEC), Via Granarolo 64, 48018 Faenza, (RA), Italy. E-mail: anna.costa@istec.cnr.it, magda.blosi@istec.cnr.it*

[b] *Department of Biomedical, Surgical and Dental Sciences, University of Milan, Via Pascal 36, 20133 Milano, Italy*

[c] *Department of Pharmacological and Biomolecular Sciences, University of Milan, Via Balzaretti 9, 20133 Milano, Italy*

[d] *Department of Biomedical Sciences for Health, University of Milan, Via Pascal 36, 20133 Milano, Italy*

[e] *National Research Council of Italy, Institute of Intelligent Industrial Technologies and Systems for Advanced Manufacturing (CNR-STIIMA), Corso Pella 16, 13900 Biella, Italy*

[f] *Department of Applied Physics, KTH Royal Institute of Technology, SE106 91 Stockholm, Sweden*

† Electronic supplementary information (ESI) available. See DOI: https://doi.org/10.1039/d2en00178k

The proliferation and spread of resistant microorganisms pose lethal threats to humans and animals. Just in the last two decades, after the severe acute respiratory syndrome coronavirus (SARS-CoV) and the Middle East respiratory syndrome coronavirus (MERS-CoV), SARS-CoV-2 emerged as the third highly pathogenic human coronavirus; SARS-CoV-2 alone has caused the recent COVID-19 disease global pandemic.[1] Protection from these viruses and bacteria entails two complementary strategies: 1) the inhibition of the development of the diseases that follow infections, and 2) the prevention of the infection itself by minimizing contact with active pathogens. Vaccination and antiviral therapies are considered optimal approaches to minimize the consequences of viral infections; these pharmacological solutions, however, cannot guarantee long-term immunity

This journal is © The Royal Society of Chemistry 2022

Environ. Sci.: Nano, 2022, **9**, 4295–4304 | **4295**

due to intrinsic uncertainties in their efficacy and to rapid mutations of the pathogens; in addition, unavoidable malfunctions in the massive production and distribution of drugs and vaccines do not always ensure their immediate availability. The inactivation of the pathogens before they can reach humans and animals becomes then crucial to counteract the development of viral and bacterial diseases. On this line, in this paper, we report the antiviral and antibacterial activities of a particular class of Ag nanoparticles stabilised in a cellulose-based matrix[2] (Ag-HEC NPs) and define the condition of their highest efficacy in different applications.

The antimicrobial activity of metals such as silver, gold and copper has been known for centuries,[3–6] and the current emergence of bacteria resistant to antibiotics has spurred renewed interest in these materials;[7–10] in particular, nanoparticles composed of these materials have been reported to exhibit extraordinary efficacy against virus infection and replication.[11–18] The full exploitation of metal nanoparticles as effective antimicrobial agents, however, faces two challenges: 1) the environmentally sustainable production of massive amounts of nano-enabled antimicrobials, and 2) the control of toxicity that antimicrobial activity may induce. The same unique properties of nanomaterials, in fact, that promise to transform and improve currently available technologies may involve hard-to-predict risks to human health and the environment.[19–21] It must be also mentioned that existing nanotechnology solutions suffer from a lack of a clear and scientifically sound quality and efficacy validation pathway that, starting from the design stage of the product development, ensures functionality, safety, sustainability and regulatory compliance (or, preparedness).[22] To this purpose, knowledge from EU nano-safety projects can really be helpful for defining decision criteria guiding the selection of the best nanomaterials and manufacturing processes. An example is reported in previous papers,[23,24] suggesting a strategy for a safe by design (SbD) use and verification of Ag NP based coatings.

As reported by Costa and Blosi,[2] Ag-HEC NPs can be produced by an up-scalable eco-friendly process. The mechanisms of antimicrobial activity of Ag NPs, however, are not yet fully understood; data suggest that differences in structural, physical, and chemical characteristics lead to the observed broad variability of antimicrobial activity of Ag NPs.[14,24–29] Among methods of green synthesis of silver nanoparticles, polysaccharides are used as capping agents, or in some cases, can serve as both reducing and capping agents. Some examples of synthesis of cellulose-AgNPs are reported in the literature; nevertheless, they require thermal treatments and work at very low concentration of Ag (lower than two orders of magnitude in comparison with the proposed synthesis).[30] The alternative use of a quaternised hydroxyethyl cellulose takes advantage of the presence of ionic ammonium groups that are expected to improve the coordination capacity of cellulose surrounding the as-synthesised Ag-nuclei and to add the intrinsic antimicrobial and adhesive activities of the polymeric quaternary

ammonium compounds to the designed antimicrobial nano-phases.[31] To assess the use of Ag-HEC, in this paper we focus on the assessment of the antimicrobial activity against SARS-CoV-2 and *Escherichia coli* in three different forms (representative of potential applications): i) dispersed in water, ii) deposited on fabrics, and iii) embedded in mucose-like hydrogels (3D-hydrogel scaffolds). Results from this analysis will be used to establish the conditions that minimize harmful risks preserving the antiviral and antibacterial activities of the Ag-HEC NP-based substrates.

2. Results and discussion

2.1. Physicochemical characterization

Ag-HEC nanosol. The conversion of Ag salt to metal Ag occurred with high efficiency (~99%), as revealed by the low residual concentration of Ag^+ (Ag^+/Ag tot = 0.07%) in equilibrium with the metal phase in water. The quaternized hydroxyethylcellulose (HEC) acts both as a chelating and reductive agent toward the silver ions. When the alkaline solution is added, a gel forms immediately, assuming a dark brown color due to the formation of Ag_2O and to the first Ag nuclei and turning to brown-yellow after about 24 hours with a decrease of viscosity, till a complete formation of a Ag NP dispersion. The alkaline condition generates new reducing aldehydic end groups in HEC macromolecules[30] which promote the reduction of Ag ions to nanoparticles nucleated and grown into the polymer acting as a chelating agent as well. HEC/Ag = 5.5 and NaOH/Ag = 2.8 were identified as the optimal molar ratios to control reduction, nucleation and growth phenomena and ensure total Ag^+ conversion, particle size homogeneity and long colloidal stability over time. The metal phase consisted of nanoparticles with spheroid morphology, with diameter in the range of 2–20 nm (mean diameter 9 nm ± 1 nm) as revealed by TEM images (Fig. 1); an evident absorption band in the surface plasmonic resonance centered around 410 nm (Fig. S1†) confirmed these results. Let us observe that these sizes fall in the range of sizes for which a high antibacterial activity has been reported.[32,33] The hydrodynamic diameter assessed by DLS refers not only to the inorganic particle, but to the particle comprising the chelating polymer and representing the kinetic unit in suspension. For this reason, AgNPs embedded into HEC polymeric chains exhibited diameters much larger than the real ones measured by TEM. The positive surface charge is in line with the cationic quaternized hydroxyethyl cellulose adsorption on the particles' surface.

6-month aging does not alter the colloidal stability of the AgHEC nanosol, the sample shows a lower hydrodynamic diameter and polydispersity index (PDI), and is characterized by a lower Ag salt to Ag metal degree of conversion, as the reaction was completed during the storage time (Table 1). In order to characterize the samples also in culture media where the cytotoxicity is measured, we diluted the Ag-HEC nanosol in DMEM + FBS 10%, and verified the expected formation of a negative corona[29,34,35] (negative zeta potential), with an

4296 | *Environ. Sci.: Nano*, 2022, **9**, 4295–4304

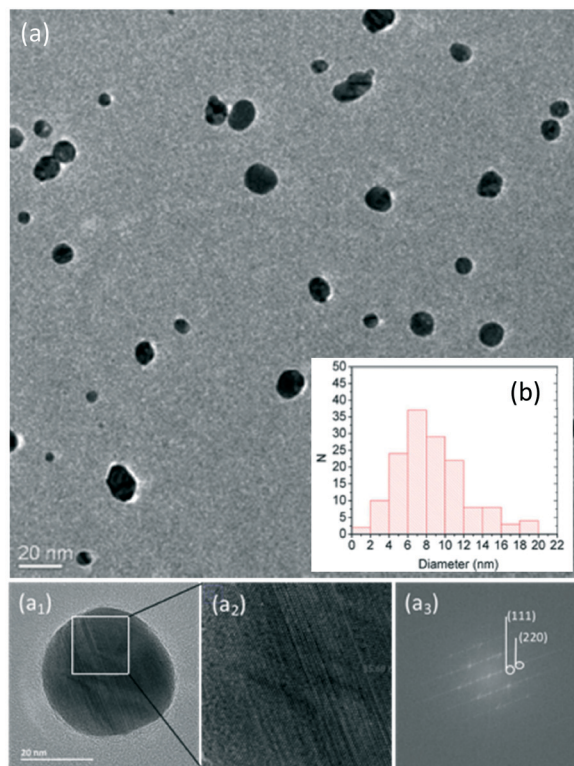This journal is © The Royal Society of Chemistry 2022

Fig. 1 TEM micrographs (a) and size distribution (b) of as-synthesized Ag-HEC NPs. TEM micrograph of Ag NPs at higher magnification (a1); close up showing lattice fringes (a2); and (a3) FFT indexed to cubic Ag (ICDD card no: 00-001-1167).

increase of the percentage of the ionic fraction at the equilibrium, due to the complexation of metal ions with proteins.[36]

A high degree of crystallinity of the Ag NPs can be revealed from Fourier-transform of TEM images that exhibited, in fact, visible lattice fringes (Fig. 1-a2). Some of the points on the FFT are indexed to cubic Ag lattice planes, which are marked with the corresponding indices on the FFT micrograph (Fig. 1-a3).

Ag-HEC coated fabrics. ICP-OES analyses performed on the Ag-HEC coated fabrics revealed an inhomogeneous distribution of Ag NPs on the surfaces, with a mass of Ag per unit mass of textile that varies from 0.028 to 0.21 mg g^{-1} among three different sample zones. This inhomogeneous distribution of Ag is visible (yellow sample) in optical photographs of fabrics spray-coated with Ag-HEC reported in Fig. S2.† This inhomogeneous distribution has been already

reported for spray-coating of nanoparticles and is the same for the three different textiles.[37]

Ag-HEC 3D-hydrogel scaffolds. The composition of Ag-HEC hydrogels is detailed in Table S1.† The Ag concentration in the wet hydrogels was 0.025 wt%. After water removal by freeze-drying, we obtained dried hydrogels, tested as scaffolds, with Ag contents ranging from 1.37 wt% (for Ag-HEC/K-Carr and Ag-HEC/Agar) to 1.07 wt% (for Ag-HEC/K-Carr/Chit and Ag-HEC/Agar/Chit). Fig. S3† shows pictures of freeze-dried samples. For Ag-HEC hydrogels, both the swelling capacity and water dissolution, with reference to the dried gel weight, were measured and are reported in Table 2.

The K-carrageenan-based hydrogel showed the smallest swelling capacity and the highest degree of dissolution in water, whilst the addition of chitosan or agar improved both the swelling capacity (i.e., the amount of water that the hydrogel can absorb without damage) and the stability in water.

2.2. Cytotoxicity tests

The in vitro cytotoxicity of the Ag-HEC nanosol was investigated by the MTT assay and compared to that of chloroquine (CQ), a well-known antibacterial and virucidal drug. Exposing the Vero cell cultures to a series of Ag-HEC nanosols and CQ at different concentrations yielded values of CC50 and CC10, which are the concentrations that lead to 50% and 10%, respectively, reduction of cell viability (Table 3 and Fig. 3).

Based on these data, the lowest cytotoxic concentration of the Ag-HEC nanosol was found to be 126 ± 28 µg mL^{-1}. We observe that this value is well below 1 wt% (10 000 µg mL^{-1}), that is the maximum limit suggested by the scientific committee on consumer safety (SCCS),[38] reported in the latest scientific advice on the safety of nanomaterials and cosmetics; so, considering the hypothesized application and based on the results of cytotoxicity tests, we can estimate concentrations up to 300 µg mL^{-1} are applicable and can be used to compare the antiviral activity of Ag NPs with chloroquine.

2.3. Antiviral activity

Antiviral activity of Ag-HEC nanosol. The antiviral activity of the Ag-HEC nanosol was tested following two different schemes of exposure: 1) exposure of cells to a mixture of Ag-HEC nanosol and virus [(Ag-HEC nanosol + virus) + cells], and 2) addition of the Ag-HEC nanosol to cells that have been infected with virus, [(virus + cells) + Ag-HEC nanosol].

Table 1 Summary of the Ag-HEC nanosol's physicochemical properties

Sample	d_{DLS} (nm)	PDI	Zeta potential (mV)	pH	Ag$^+$/Ag tot (%)
Fresh Ag-HEC (MilliQ water)	328 ± 52	0.4	17.5 ± 2	12.2 ± 0.1	0.07 ± 0.02
Aged[a] Ag-HEC (MilliQ water)	241 ± 9	0.3	6.3 ± 0.4	12.9 ± 1.4	0.02 ± 0.01
Ag-HEC (DMEM + FBS 10%)	93 ± 3	0.6	−1.9 ± 0.5	8.5 ± 0.2	0.20 ± 0.10

The Ag-HEC nanosol has been diluted in MilliQ water and in culture medium (50 µg mL^{-1}, 1 h of exposure). [a] 6 months of storage at 4 °C.

This journal is © The Royal Society of Chemistry 2022

Environ. Sci.: Nano, 2022, **9**, 4295–4304 | **4297**

Table 2 Ag-HEC hydrogels' swelling capacity and dissolution in water

Sample	Wd (g)	Swelling (%)	Dissolution (%)
Ag-HEC/K-Carr	0.81	20.8	13.4
Ag-HEC/Agar	0.42	36.5	0.1
Ag-HEC/K-Carr/Chit	0.44	32.7	7.0
Ag-HEC/K-Carr/HEC	0.44	37.4	11.3

Table 3 CC50 and CC10 of the Ag-HEC nanosol and CQ

	Ag (μg mL^{-1})	CQ (μM)^a
CC50	275.7 ± 64.5	95.3 ± 18.0
CC10	126.0 ± 27.8	20.9 ± 4.4

^{a} MW CQ = 319.87 g mol^{-1}; therefore CC50 = 30.5 μg mL^{-1} and CC10 = 6.7 μg mL^{-1}.

The second scheme, adopted also for chloroquine, did not lead to any observable effect, while we detected a reduction of viral activity in the first case. These observations suggest that Ag NPs interfere directly with the virus and prevent the contact between active SARS-CoV-2 and the cells.

Table 4 summarizes the results obtained by qRT-PCR expressed in terms of difference in the cycle threshold ΔCt and viral load (as the average of minimum three experiments), and the percentage of SARS-CoV-2 replication. The Ag-HEC nanosol at the highest concentration of 300 μg mL^{-1} showed an antiviral activity comparable with CQ at 16.7 μM that was tested following the second scheme of exposure ([virus + cells] + CQ). These results reveal different mechanisms of antiviral action for Ag-HEC NPs and CQ; Ag-HEC NPs inactivate the virus before it penetrates into the cells, whilst CQ affects the replication steps once the virus has entered into the host cell. The details of the mechanism of antiviral action of Ag NPs are not yet fully clarified; nevertheless the most accredited hypothesis, consistent with our observations, assumes that, outside the cell, viruses may adsorb on the surface of NPs, which, in turn, mask the receptor and binding domain (spike proteins).[39,40] In
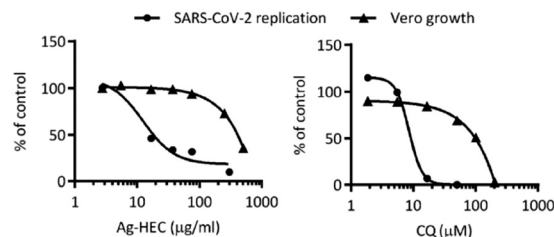

Fig. 2 Values of ΔCt for SARS-CoV-2 *vs.* concentration of Ag-HEC nanosol (blue) and chloroquine (red).

Fig. 3 SARS-CoV-2 viral load data (copies per μL) and cell viability data (OD 550-650 nm) were normalized *versus* untreated infected controls according to the following formula: % control = 100 × (viral load or OD treated sample/viral load or OD untreated control). Data were plotted as a function of the Ag-HEC nanosol and CQ concentration and curve fitting was obtained by non-linear regression analysis using a four-parameter logistic method (software GraphPadPrism 6). The results are the mean of three independent experiments.

contrast, CQ can act at the early stage of virus replication, blocking intracellular signaling and affecting virion assembly and budding.[41]

Fig. 2 reports the variation of ΔCt for the Ag-HEC nanosol at different concentrations. It can be noted that the antiviral activity remained approximately constant at concentrations below the CC10 ($\sim$150 μg mL^{-1}) and exhibited an abrupt increase at 300 μg mL^{-1}, a concentration higher than the CC50 (275 μg mL^{-1}) for cytotoxicity. We recall that the cytotoxicity of the Ag-HEC nanosol is partially due to the release of Ag$^+$, which induces the denaturation of proteins that regulate ATP production and DNA replication, but also to the generation of radical oxygen species (ROS) that break down membrane and mitochondrial function.[25,42]

Most likely, at concentrations larger than CC50, a synergistic effect of inactivation of the binding domain of the virus by the Ag NPs[43] and cytotoxicity induced by the release of Ag$^+$ occurs and leads to the abrupt increase of antiviral activity around 300 μg mL^{-1} of Ag-HEC.[32]

The virucidal activity of the Ag-HEC nanosol was confirmed by the plaque assay in the concentration range of 18 μg mL^{-1} to 150 μg mL^{-1} (Table 6), which revealed a reduction of SARS-CoV-2 infectivity by $\sim$50% at 150 μg mL^{-1}.

The objective of the investigation of cytotoxicity and virucidal activity was to define the concentrations of the Ag-HEC nanosol that can be used in antiviral application with no residual toxicity; this amount can be estimated from the selectivity index (SI), that is, the ratio of cytotoxicity to biological reactivity, in the present study given by CC50/IC50 (the antiviral 50% inhibition concentration). Fig. 3 shows the effect of concentration of the Ag-HEC nanosol and CQ on the SARS-CoV-2 viral load and Vero cell viability, and Table 6 reports the values of the cytotoxicity and antiviral activity and the corresponding values of selectivity index for the Ag-HEC nanosol and chloroquine.

The selectivity index for the Ag-HEC nanosol was found to be above the limit ($\geq$10) assumed for promoting its effective and safe use.[44] Furthermore, a selectivity index higher than that of CQ clearly suggested a broader range of safe
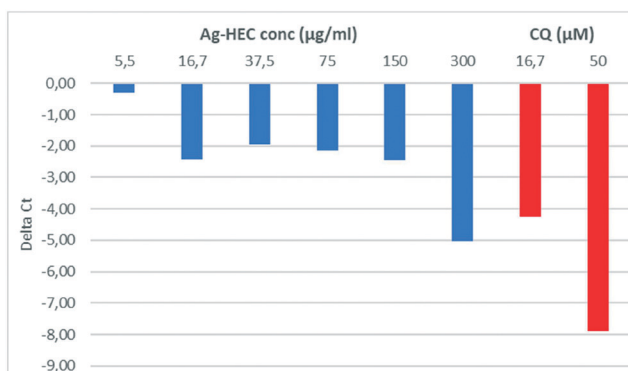
4298 | *Environ. Sci.: Nano*, 2022, **9**, 4295–4304

This journal is © The Royal Society of Chemistry 2022

Table 4 Antiviral activity of the Ag-HEC nanosol against SARS-CoV-2 expressed as mean ΔCt, mean viral load, and percentage of replication. The HEC sample corresponds to the blank suspension containing all the synthesis additives, except for AgNPs

Concentration of Ag-HEC nanosol ($\mu g\ mL^{-1}$)	ΔCt	Viral load (copies per μL)	% SARS-CoV-2 replication
300	-5.03 ± 1.20	$5.11 \times 10^{8a} \pm 6.95 \times 10^5$	7.27
150	-2.46 ± 0.31	$2.19 \times 10^{9a} \pm 4.49 \times 10^5$	31.17
75	-2.14 ± 0.33	$1.64 \times 10^{9a} \pm 4.30 \times 10^5$	23.35
37	-1.96 ± 0.40	$1.75 \times 10^{9a} \pm 3.78 \times 10^4$	24.95
16.7	-2.43 ± 0.02	$2.39 \times 10^{9a} \pm 2.25 \times 10^4$	34.09
5.5	-0.31 ± 0.20	$5.18 \times 10^9 \pm 5.12 \times 10^4$	73.89
300 (HEC_blank)	0.17 ± 0.02	$7.59 \times 10^9 \pm 6.01 \times 10^5$	100
37.5 (HEC_blank)	-0.21 ± 0.08	$6.70 \times 10^9 \pm 4.40 \times 10^5$	95.30
Chloroquine (control) 50 μM	-7.90 ± 2.18	$1.80 \times 10^{7a} \pm 4.62 \times 10^2$	0.25
Chloroquine (control) 16.7 μM	-4.24 ± 1.04	$4.89 \times 10^{8a} \pm 2.23 \times 10^4$	6.90
No treatment	0	$7.03 \times 10^{9a} \pm 2.35 \times 10^5$	100

Data for the difference in cycle threshold (ΔCt) and viral load are mean values $\pm$ standard deviations of, at least, three experiments. $^a = p < 0.05$.

concentration of the Ag-HEC nanosol to be used in application (Table 5).

Antiviral activity of Ag-HEC fabrics and scaffolds. Finally, the virucidal activity against SARS-CoV-2 was also evaluated for the virus exposed to immobilized Ag NPs, in the form of coating (PPNW/PVA/Ag-HEC fabric) and scaffold (Ag-HEC/K-Carr hydrogel) (Table 7).

The virus activity on Ag-HEC-loaded fabrics and scaffolds was reduced by about 33% and 44%, respectively, when compared with the untreated substrates, pointing out that although Ag NPs were immobilized on a matrix the antiviral action capability was kept. It is important to stress that withdrawing the virus from the hydrogel scaffolds after exposure was difficult, indicating a potentially synergistic effect against virus replication due to the adsorption/entrapping action of the hydrogel combined with the de-activation by Ag NPs.

These results are also encouraging from the perspective of promoting the safe use of Ag-HEC through the two potential applications suggested by the two nano-enabled products (fabrics to be used in personal protective equipment and hydrogel as a base for protective molecular masks). In fact, as schematized in Fig. S4,† the Ag amount corresponding to the reference dose for oral exposure of bulk Ag, as suggested by the EPA (350 μg person^{-1} day^{-1}),[45] is potentially delivered by a large area of fabrics (from A3 to A1 formats, due to the inhomogeneity of Ag deposited) or by 1/3 of the volume of the hydrogel scaffold produced, so the real dose that can be

extrapolated, in the hypothesized condition of use, will be reasonably below such limit.

2.4. Antibacterial activity of Ag-HEC fabrics and scaffolds

The results of antibacterial tests performed on Ag-HEC coated fabrics are reported in Table 8. The tests were performed also after abrasion or washing (laundering cycles) in order to assess washing and mechanical resistance.

All the Ag-HEC coated fabrics showed a substantial, and in some cases complete, reduction of *Escherichia coli* after 1 hour. These results revealed also a strong adhesion of Ag NPs to the hydroxyethyl cellulose matrix (HEC) which led to efficient antibacterial activity after washing. Table 9 reports the results for antibacterial activity of the 3D-hydrogel scaffolds, which, by loading with Ag-HEC, exhibited a complete removal of *E. coli*.

3. Materials and methods

3.1. Synthesis of Ag-HEC and preparation of the relative nanosol

Ag NPs can be prepared by an efficient (reaction yield, 99.9%) and scalable synthetic protocol patented by Costa and Blosi,[46] which leads to a concentrated nanosol (0.1–0.5 wt% Ag) stable for 12 months. In short for Ag-HEC 0.5 wt%, a 0.05 M solution of silver nitrate (Sigma-Aldrich, USA) was added to a solution of quaternized hydroxyethyl cellulose, HEC (Dow Chemical, USA), with a HEC/Ag molar ratio of 5.5; the resulting solution was stirred for 5 minutes. A 1 M solution of NaOH (Sigma-Aldrich, USA) was then added dropwise to the reaction mix up to a NaOH/Ag molar ratio of 2.8 to form a gel. Formation of metal Ag from reduction of Ag ions leads to a black-brown color of the gel, which, however, turned into a yellowish brown low viscosity dispersion after 24 hours.

This gel, composed of Ag NPs dispersed in a matrix (network) of quaternized hydroxyethyl cellulose, can be easily dissolved in water to obtain nanosols of suitable

Table 5 Antiviral activity (IC50), cytotoxicity (CC50, CC10) and selectivity index of the Ag-HEC nanosol and CQ

Compound	IC50	CC50	CC10	SI
Ag-HEC ($\mu g\ mL^{-1}$)	12.42	275.7 ± 64.5	126.0 ± 27.8	22.2
CQ (μM)	11.30	95.3 ± 18.0	20.9 ± 4.4	8.43

Data are the means $\pm$ SD of three independent experiments performed in duplicate; SI = selectivity index = CC50/IC50.

This journal is © The Royal Society of Chemistry 2022

Environ. Sci.: Nano, 2022, **9**, 4295–4304 | **4299**

Table 6 Virucide activity of the Ag-HEC nanosol and CQ expressed as the mean number of plaques mL^{-1}, and as the percentage of replication

| | Untreated infected cells | Mean PFU mL^{-1} ± SD (% of replication) | | | |
		18 µg mL^{-1}	37 µg mL^{-1}	75 µg mL^{-1}	150 µg mL^{-1}
Ag-HEC nanosol	59.38[a] ± 6.86 (100%)	47.92 ± 6.93 (80.7%)	39.17[a] ± 5.60 (65.97%)	44.58[a] ± 6.52 (75.09%)	27.71[a] ± 3.03 (46.67%)
	Untreated infected cells	1.9 µM	5.6 µM	16.7 µM	50.0 µM
CQ	85 (100%)	73.3 (86.2%)	54.3 (63.8%)	0 (0%)	0 (0%)

[a] = $p < 0.05$.

Table 7 Virucide activity of PPNW/PVA/Ag-HEC fabric and Ag-HEC/K-Carr hydrogel scaffold, expressed as the mean number of plaques per mL and as the percentage of replication

| | Mean PFU mL^{-1} ± SD (% SARS-CoV-2 replication) | |
	Untreated infected	Treated infected
PPNW/PVA/Ag-HEC fabric	49.38[a] ± 5.66 (100%)	32.71[a] ± 3.54 (66.25%)
Ag-HEC/K-Carr hydrogel scaffold	112[a] ± 1.74 (100%)	62.75[a] ± 3.04 (56.03%)

[a] = $p < 0.05$.

concentration; the physicochemical characterization of Ag-HEC nanosols are described in the ESI.†

3.2. Deposition of the Ag-HEC nanosol on different types of fabric and its resistance to washing and abrasion

We used 5 mL of nanosol to deposit, by spray coating, Ag-HEC NPs on textile substrates. To improve the adhesion of Ag-HEC NPs, we added poly(vinyl alcohol), PVA, with a molecular mass of 130 kDa and hydrolysis degree >99% (Sigma-Aldrich, USA), to the nanosol. PVA was dissolved at a concentration of 1.0 wt/vol% in water and kept for 2 hours under stirring at 90 °C. The polymeric solution was cooled down overnight under stirring, then the Ag-HEC nanosol at 0.1 wt% Ag content was added with a 1:1 volume ratio. The resulting PVA/Ag-HEC NPs dispersion was stirred for 2 hours to ensure homogeneity. This dispersion was used to deposit Ag-HEC NPs on three different types of fabric composed of

the most used polymeric fibers: 1) spunbonded non-woven polypropylene (PPNW) composed of 16 µm fibers, with an areal density of 23 g m^{-2}; this type of fiber is used in clothing products and in many other applications that include automotive, building products, filtration, and lamination; 2) polyamide (PA 6,6) fabric, with a tread count of 44 × 36 yarns cm^{-1} and 59 g m^{-2} areal density; PA 6,6 finds applications in the clothing industry (e.g., fashion, technical, sport, lingerie); and 3) ISO 105 F04 polyethylene terephthalate (PET) fabric; PET yarn is used to produce clothes and carpets. The coated fabrics were then oven dried at 80 °C for 2 min.

We tested the antiviral and antibacterial activities of 20 cm × 20 cm square samples of each coated fabric.

The resistance of the functionalized samples against washing and abrasion was also assessed; washing was assessed, according to ISO 105-C06 A1S, at 40 °C with an ECE detergent and repeated washing cycles of 30 min, while 1000-cycle abrasion tests were performed according to ISO 12947-2 using a Martindale apparatus at 12 kPa loading.

3.3. Embedding of Ag-HEC NPs into hydrogel-based scaffolds

For the preparation of Ag-HEC hydrogel-based scaffolds, the Ag-HEC nanosol (0.5 wt% Ag) was mixed with aqueous solutions of different biopolymers (K-carrageenan, agarose, chitosan) in the amounts reported in Table S1.† The Ag-HEC nanosol was heated up to 90 °C under magnetic stirring and the biopolymeric solutions were added to the Ag-HEC nanosol dropwise and kept at 90 °C for a further 20 min. After that, the suspension was cast into silicon molds and allowed to cool to room temperature for 4 hours. The gelled samples were freeze-dried and easily removed from the molds. 3 cm × 3 cm hydrogel squares (0.5 cm thickness, mass about 0.1 g) were thus prepared. Hydrogels without added Ag were also produced and tested as negative control blanks

Table 8 Antibacterial tests performed on Ag-HEC coated fabrics. Fabrics coated by HEC refer to the application of the blank suspension containing all the synthesis additives, except for AgNPs

Ag-HEC coated fabrics	Bacterial reduction%
PVA (reference)	27.2 ± 1.5
PPNW/PVA/HEC (blank)	15 ± 1.0
PA 6,6/PVA/HEC (blank)	15 ± 1.0
PET/PVA/HEC (blank)	15 ± 1.0
PPNW/PVA/Ag-HEC	100
PA 6,6/PVA/Ag-HEC	100
PET/PVA/Ag-HEC	100
PA 6,6/PVA/Ag-HEC after 1000 abrasion cycles	95.8 ± 0.9
PA 6,6/PVA/Ag-HEC after 1 laundering	85.4 ± 1.6
PA 6,6/PVA/Ag-HEC after 10 launderings	91.2 ± 2.9
PET/PVA/Ag-HEC after 1000 abrasion cycles	99.0 ± 0.3
PET/PVA/Ag-HEC after 1 laundering	99.4 ± 0.6
PET/PVA/Ag-HEC after 10 launderings	84.7 ± 5.4

Table 9 Antibacterial tests performed on Ag-HEC 3D-hydrogel scaffolds

Sample	Weight (g)	Conc. Ag (wt%)	Bacterial reduction (%)
Blank 1 (K-Carr/HEC/Chit)	1.08	0.00	0
Blank 2 (K-Carr/HEC)	0.94	0.00	0
Ag-HEC/K-Carr/Chit	1.12	1.07	100
Ag-HEC/K-Carr	1.27	1.37	100
Ag-HEC/Agar/Chit	1.10	1.07	100
Ag-HEC/Agar	0.87	1.37	100

(Blank 1 and Blank 2). Methods for the determination of the swelling capacity and dissolution in water (stability) of the hydrogels are described in the ESI.†

3.4. Cytotoxicity of the Ag-HEC nanosol and comparison with chloroquine

We tested the cytotoxicity of the Ag-HEC nanosol and chloroquine, the reference drug, by the MTT assay in Vero cells (ATCC-CCL81-monkey kidney epithelial cells). Before testing, cells were maintained in DMEM supplemented with 10% heat-inactivated fetal calf serum, 2 mM glutamine, 100 units mL^{-1} of penicillin, and 100 μg mL^{-1} of streptomycin. Cytotoxicity was measured on cells seeded into 96-well plates at a concentration of 1×10^4 cells per well. After incubation for 24 hours, cells were treated with serial 4-fold dilutions of the Ag-HEC nanosol (from 500 to 0.5 μg mL^{-1}), or chloroquine (from 200 to 1.6 μM) (tested as positive control), by maintaining a final volume of 200 μl. After incubation for 72 hours at 37 °C in 5% CO_2, cell viability was measured by the MTT assay.[47] The absorbance was measured spectrophotometrically at a test wavelength of 550 nm and a reference wavelength of 650 nm, using a Synergy 4 microplate reader (Biotek, GE). The percentage of viable cells was calculated using untreated cells as a control (100% viability) using the formula:

$$(\%) = 100 \cdot \frac{\text{(sample abs)}}{\text{(control abs)}} \qquad (1)$$

From this equation, we estimated, by the Gene5 software, the CC50, that is, the concentration of Ag-HEC NPs, or chloroquine, that reduced the viability of Vero cells by 50% with respect to the untreated cells. This parameter is very useful in comparing the effects of different compounds on the response of cell culture: in principle, the lower the value of CC50, the more cytotoxic the compound.

3.5. Biological activity

Antiviral activity of the Ag-HEC nanosol. For testing the antiviral activity of the Ag-HEC nanosol, Vero cells were seeded into 96-well plates at a density of 1.3×10^4 cells per well and incubated for 24 h at 37 °C in 5% CO_2. SARS-CoV-2 virus was isolated from nasal–pharyngeal swabs as described in the ESI.† The Ag-HEC nanosol was incubated with the

virus (corresponding to a MOI of 0.05; 1000 PFU per well) at Ag concentrations of 300, 150, 75, 37, 16.7, and 5.5 μg mL^{-1}, for 1 hour at room temperature, then cells were infected and incubated for 2 hours at 37 °C in 5% CO_2.

In all the experiments, chloroquine was used as a control drug, although incubated according to a different scheme: after removal of the virus inoculum, the cells were treated with only the medium (control) or the medium containing chloroquine (from 50 to 1.9 μM), and incubated for 72 hours at 37 °C, 5% CO_2.

The scheme used for chloroquine was also used with the Ag-HEC nanosol, at the same dose range reported above, in order to check if differences in the mechanism of action occurred by inverting the order of exposure. Therefore, the following two cases were considered for the Ag-HEC nanosol: [Ag-HEC nanosol + virus] + cells (1st case) or [virus + cells] + Ag-HEC nanosol (2nd case).

The antiviral activity of the Ag-HEC nanosol against SARS-CoV-2 was monitored by qRT-PCR.

Antiviral activity of fabrics coated with Ag-HEC NPs. For testing the antiviral activity of fabrics loaded with Ag-HEC NPs, a total of 150 μL of the virus inoculum was deposited on the Ag-HEC coated fabric samples (average weight 0.07 ± 0.02 g) following the ISO18184 International standard protocol. After exposure, the inoculum was washed out with 20 mL of cell growth medium. The resulting washing medium was 10-fold serially diluted before measuring the virucidal activity in triplicate by a plaque assay, as described in section 2.3, and reported as the percentage of viral replication, considering the replication on untreated fabrics as 100%. Uncoated fabrics were used as negative controls.

Antiviral activity of 3D-hydrogel scaffolds loaded with Ag-HEC NPs. For testing the antiviral activity of hydrogel scaffolds loaded with Ag-HEC NPs, a total of 150 μL of the virus inoculum was deposited on freeze-dried hydrogels (average weight 0.11 ± 0.02 g), following ISO21702, and dried at room temperature for 1 h. As for the coated fabrics, the antiviral activity of Ag-HEC loaded hydrogel scaffolds was estimated from triplicate analysis of a plaque assay, as described in section 2.3, and reported as the percentage of viral replication, considering the replication on untreated scaffolds as 100%. Free-Ag scaffolds were used as negative controls.

Virucidal activity *via* qRT-PCR. Virucidal activity was quantified, by specific quantitative real-time polymerase

This journal is © The Royal Society of Chemistry 2022

Environ. Sci.: Nano, 2022, **9**, 4295–4304 | **4301**

chain reaction (qRT-PCR), from the number of copies of viral RNA isolated from the cell supernatants using the Nucleospin RNA virus kit (MAcherey Nagel, Germany). Results were expressed as:

• The difference in cycle threshold (Ct) values of the supernatant of untreated and treated infected cells (ΔCt = Ct of the supernatant of untreated – Ct of the supernatant treated infected cells); Ct is inversely correlated to the amount of the target; ΔCt = 3 corresponds to an average decrease of viral load of 1 log;[48]

• The SARS-CoV-2 load expressed as copies per mL;

• The percentage of replication compared to the untreated control calculated based on copies per mL.

Virucidal activity *via* a plaque assay. In order to verify the virucidal activity of the compounds (Ag-HEC coated fabrics or loaded hydrogel scaffolds), a plaque assay was conducted after the virus + compound inoculum (400 μL per well) was put on the cells, plated in a 96-well plate. After 2 h the inoculum was removed and the cells were covered with 0.3 wt% agarose dissolved in cell medium and incubated for 72 h at 37 °C with 5% CO_2. Cells were fixed with 4 wt% formaldehyde solution and, after agarose removal, stained with methylene blue. Plaques were counted and results are expressed as PFU mL^{-1} and as log of the difference between untreated infected cells and treated infected cells.

Statistical analyses for virucidal activity tests. All data obtained were analyzed with GraphPad Prism 7.0 software. Statistical analyses for the comparison of uninfected or infected cells were conducted using unpaired Student's *t*-test. A two tailed-*p* value < 0.05 was considered statistically significant.

Antibacterial assay. The antibacterial activity of Ag-HEC fabrics and scaffolds was measured by following the standard methodology ASTM E2149-13 ("Standard test method for determining the antimicrobial activity of antimicrobial agents under dynamic contact conditions") against *Escherichia coli* ATCC 11229 (Gram negative). The tests were performed by diluting the bacterial inoculum up to 1.5–3.0 × 10⁵ CFU mL^{-1}. 1 g of the substrate (Ag-HEC fabric or scaffold) was immersed in 50 mL of inoculum and kept under stirring (190 rpm) for 1 h at room temperature. After that, 1 mL of solution was incubated for 24 h in Yeast Extract Agar at 37 °C. The tests were performed in duplicate. The antibacterial activity was expressed as bacteria reduction (%) and calculated as follows:

$$\text{Bacteria reduction (\%)} = \frac{(B-A)}{B} \cdot 100 \qquad (2)$$

A: number of bacterial colonies in the diluted inoculum in contact with the substrate;

B: number of bacterial colonies in the diluted inoculum.

4. Conclusions

In this study, we presented an effective antimicrobial Ag NP technology prepared by an eco-friendly and easily scalable synthetic route entirely carried out at room temperature in the presence of benign reagents; the method yields Ag NPs embedded in a hydroxyethyl cellulose matrix (Ag-HEC NPs).

Antibacterial and antiviral activities were tested against *Escherichia coli* and SARS-CoV-2 respectively, with the latter one being isolated from a nasal–pharyngeal swab. We proved the antiviral and antibacterial properties of these Ag-HEC NPs in three different forms: dispersed in water (droplet environment), deposited on textile substrates (surface environment), and embedded in a mucose-like hydrogel (biological target environment).

Our findings pointed out an actual enhanced risk/benefit profile of Ag-HEC NPs with respect to chloroquine, as supported by a selectivity index > 10, the recommended limit set for a selective bioactive sample.[49]

The antiviral activity in the presence of Ag-HEC NPs was set around 30% of SARS-CoV-2 replication passing from very low Ag concentration up to 150 μg mL^{-1} (below the no-cytotoxicity limit), whilst it abruptly increased at the highest tested concentration (300 μg mL^{-1}), close to the CC50 value, where only 7% of the virus replicated. Unlike what happened with chloroquine, a pre-incubation of Ag-HEC with SARS-CoV-2 is required for efficient inhibition of SARS-CoV-2 replication. This result supports the existence of two distinct antiviral mechanisms: one (for Ag NPs) occurring before virus penetration in the cells, with the second (for CQ), occurring after the virus has entered into the host cell, affecting replication steps.[39]

The mucose-like hydrogels loaded with Ag NPs showed very promising antibacterial and antiviral properties. In addition to bacteria and virus de-activation, it was observed for the hydrogels a marked sorbent capability which enabled a mechanical entrapment of the virus. Finally, also Ag NPs immobilized on the textile substrate showed the capacity to inhibit virus replication, although a full clarification of the involved mechanism requires further investigations. The reduction, or suppression, of bacterial and viral activities by these different substrates supports the use of Ag-HEC as an effective antimicrobial agent for the industrial production of protective clothing or nasal molecular masks.

Author contributions

Anna Costa: conceptualization, methodology, resources, supervision, writing – original draft, writing – review & editing. Magda Blosi: conceptualization, methodology, resources, supervision, writing – review & editing. Andrea Brigliadori: investigation, methodology, resources, validation, writing – review & editing. Ilaria Zanoni: methodology, resources. Simona Ortelli: resources, validation. Felice Simeone: writing – review & editing. Serena Delbue: investigation, methodology, resources, supervision. Sarah Dalessandro and Silvia Parapini: investigation, methodology. Claudia Vineis and Alessio Varesano: investigation, methodology. Muhammet Toprak and Bejan Hamawandi: investigation, methodology. Davide Gardini:

4302 | *Environ. Sci.: Nano*, 2022, **9**, 4295–4304

This journal is © The Royal Society of Chemistry 2022

conceptualization, supervision, validation, writing – review & editing.

Conflicts of interest

The authors declare that they have no known competing financial interests or personal relationships that could have appeared to influence the work reported in this paper.

We confirm that we have given due consideration to the protection of intellectual property associated with this work and that there are no impediments to publication, including the timing of publication, with respect to intellectual property. In so doing we confirm that we have followed the regulations of our institutions concerning intellectual property.

We declare that this manuscript has not been published elsewhere in whole or in part and is not under consideration by another journal. Approval of the authors' institution has been granted to publish this work.

General statement: "There are no conflicts to declare".

References

1 Global research on coronavirus disease (COVID-19).

2 A. L. Costa and M. Blosi, *Process for the preparation of nanoparticles of noble metals in hydrogel and nanoparticles thus obtained*, 2016.

3 A. Ebrahiminezhad, M. J. Raee, Z. Manafi, J. A. Sotoodeh and G. Younes, Ancient and Novel Forms of Silver in Medicine and Biomedicine, *J. Med. Technol.*, 2016, **2**, 122–128.

4 M. Horue, M. L. Cacicedo, M. A. Fernandez, B. Rodenak-kladniew, R. M. Torres and G. R. Castro, *et al.* Materials Science & Engineering C Antimicrobial activities of bacterial cellulose – Silver montmorillonite nanocomposites for wound healing, *Mater. Sci. Eng., C*, 2020, **116**, 111152.

5 S. Song, Z. Liu, M. Aamer, L. Ding and J. Zhang, Materials Science & Engineering C Antibacterial polyvinyl alcohol / bacterial cellulose / nano-silver hydrogels that effectively promote wound healing, *Mater. Sci. Eng., C*, 2021, **126**, 112171.

6 R. Vazquez-Munoz and J. L. Lopez-Ribot, Nanotechnology as an Alternative to Reduce the Spread of COVID-19, *Challenges*, 2020, **11**(2), 15.

7 S. Behzadinasab, A. Chin, M. Hosseini, L. Poon and W. A. Ducker, *A Surface Coating that Rapidly Inactivates SARS-CoV - 2*, 2020.

8 B. Balasubramaniam, R. S. Prateek, M. Saraf, P. Kar and S. P. Singh, *et al.* Antibacterial and Antiviral Functional Materials:

9 J. Hasan, A. Pyke, N. Nair, T. Yarlagadda, K. Spann and P. K. D. V. Yarlagadda, *Antiviral Nanostructured Surfaces Reduce the Viability of SARS- CoV - 2*, 2020.

10 Y. Wang, H. Tang, D. Wu, D. Liu, Y. Liu and A. Cao, *et al.* Enhanced bactericidal toxicity of silver nanoparticles by the antibiotic gentamicin, *Environ. Sci.: Nano*, 2016, **3**, 788–798.

11 M. E. Barbinta-Patrascu, N. Badea, C. Pirvu, M. Bacalum, C. Ungureanu and P. L. Nadejde, *et al.* Multifunctional soft hybrid bio-platforms based on nano-silver and natural compounds, *Mater. Sci. Eng., C*, 2016, **69**, 922–932.

12 E. V. R. Campos, A. E. S. Pereira, O. J. L. De, L. B. Carvalho, M. G. Casagrande and L. R. De, *et al.* How can nanotechnology help to combat COVID - 19 ? Opportunities and urgent need, *J. Nanobiotechnol.*, 2020, 1–23.

13 L. Chen and J. Liang, An overview of functional nanoparticles as novel emerging antiviral therapeutic agents, *Mater. Sci. Eng., C*, 2020, **112**, 110924.

14 P. Merkl, S. Long, G. M. McInerney and G. A. Sotiriou, Antiviral Activity of Silver, Copper Oxide and Zinc Oxide Nanoparticle Coatings against SARS-CoV-2, *Nanomaterials*, 2021, **11**(5), 1312.

15 G. Pagnotta, G. Graziani, N. Baldini, A. Maso, M. L. Focarete and M. Berni, *et al.* Nanodecoration of electrospun polymeric fibers with nanostructured silver coatings by ionized jet deposition for antibacterial tissues, *Mater. Sci. Eng., C*, 2020, **113**, 110998.

16 C. Wang, X. Huang, W. Deng, C. Chang, R. Hang and B. Tang, A nano-silver composite based on the ion-exchange response for the intelligent antibacterial applications, *Mater. Sci. Eng., C*, 2014, **41**, 134–141.

17 R. Djellabi, N. Basilico, S. Delbue, S. D. Alessandro, S. Parapini and G. Cerrato, *et al.* Oxidative Inactivation of SARS-CoV-2 on Photoactive AgNPs @ TiO$_2$ Ceramic Tiles, *Int. J. Mol. Sci.*, 2021, **22**, 8836.

18 C. D. Vecitis, Antiviral-nanoparticle interactions and reactions, *Environ. Sci.: Nano*, 2021, **8**(1), 11–19.

19 C. W. Babbitt and E. A. Moore, Sustainable nanomaterials by design, *Nat. Nanotechnol.*, 2018, **13**(8), 621–629.

20 S. León-Silva, F. Fernández-Luqueño and F. López-Valdez, Silver Nanoparticles (AgNP) in the Environment: a Review of Potential Risks on Human and Environmental Health, *Water, Air, Soil Pollut.*, 2016, **227**(9), 306.

21 I. Kieffer, S. Motellier and E. Valsami-jones, *Environ. Sci.: Nano*, 2021, 806–821.

22 S. Gottardo, A. Mech, J. Drbohlavová, A. Małyska, S. Bøwadt and J. Riego Sintes, *et al.* Towards safe and sustainable innovation in nanotechnology: State-of-play for smart nanomaterials, *NanoImpact*, 2021, **21**, 100297.

23 D. Gardini, M. Blosi, S. Ortelli, C. Delpivo, O. Bussolati and M. G. Bianchi, *et al.* Nanosilver: An innovative paradigm to promote its safe and active use, *NanoImpact*, 2018, **11**, 128–135.

24 V. Marassi, L. Di Cristo, S. G. J. Smith, S. Ortelli, M. Blosi and A. L. Costa, *et al.* Silver nanoparticles as a medical

This journal is © The Royal Society of Chemistry 2022

Environ. Sci.: Nano, 2022, **9**, 4295–4304 | **4303**

device in healthcare settings: A five-step approach for candidate screening of coating agents, *R. Soc. Open Sci.*, 2018, **5**(1), 171113.

25 S. P. Deshmukh, S. M. Patil, S. B. Mullani and S. D. Delekar, *Mater. Sci. Eng., C*, 2019, **97**, 954–965.

26 S. Chernousova and M. Epple, Silver as Antibacterial Agent: Ion, Nanoparticle, and Metal, *Angew. Chem., Int. Ed.*, 2013, **52**, 1636–1653.

27 T. C. Dakal, A. Kumar, R. S. Majumdar and V. Yadav, Mechanistic Basis of Antimicrobial Actions of Silver Nanoparticles, *Front. Microbiol.*, 2016, **7**, 1831.

28 L. M. Gilbertson and J. B. Zimmerman, *Environ. Sci.: Nano*, 2021, 37–66.

29 A. Huk, E. Izak-Nau, B. Reidy, M. Boyles, A. Duschl and I. Lynch, *et al.* Is the toxic potential of nanosilver dependent on its size?, *Part. Fibre Toxicol.*, 2014, **11**, 65.

30 M. A. El-Sheikh, S. M. El-Rafie, E. S. Abdel-Halim and M. H. El-Rafie, Green Synthesis of Hydroxyethyl Cellulose-Stabilized, *J. Polym.*, 2013, **2013**, 1–11.

31 J. Shen, B. Li, X. Zhan and L. Wang, A one pot method for preparing an antibacterial superabsorbent hydrogel with a Semi-IPN structure based on tara gum and polyquaternium-7, *Polymers*, 2018, **10**(7), 696.

32 T. T. N. Dung, V. N. Nam, T. T. Nhan, T. T. B. Ngoc, L. Q. Minh and B. T. T. Nga, *et al.* Silver nanoparticles as potential antiviral agents against African swine fever virus, *Mater. Res. Express*, 2020, **6**(12), 1250g9.

33 K. Naik and M. Kowshik, The silver lining: towards the responsible and limited usage of silver, *J. Appl. Microbiol.*, 2017, **123**(5), 1068–1087.

34 B. Reidy, A. Haase, A. Luch, K. A. Dawson and I. Lynch, Mechanisms of Silver Nanoparticle Release, Transformation and Toxicity: A Critical Review of Current Knowledge and Recommendations for Future Studies and Applications, *Materials*, 2013, **6**, 2295–2350.

35 I. Lynch and K. A. Dawson, Protein-nanoparticle interactions, *Nano Today*, 2008, **3**(1), 40–47.

36 S. Ortelli, A. L. Costa, M. Blosi, A. Brunelli, E. Badetti and A. Bonetto, *et al.* Colloidal characterization of CuO nanoparticles in biological and environmental media, *Environ. Sci.: Nano*, 2017, **4**(6), 1201–1420.

37 J. D. Torrey, T. L. Kirschling and L. F. Greenlee, Processing and Characterization of Nanoparticle Coatings for Quartz Crystal Microbalance Measurements, *J. Res. Natl. Inst. Stand. Technol.*, 2015, **120**, 1–10.

38 *** Scientific Committee on Consumer Safety - SCCS. Scientific Committee on Consumer Safety SCCS - Guidance on the Safety Assessment of Nanomaterials in Cosmetics, 2021, 1–49.

39 G. W. Jones, M. P. Monopoli, L. Campagnolo, A. Pietroiusti, L. Tran and B. Fadeel, No small matter: a perspective on nanotechnology-enabled solutions to fight COVID-19, *Nanomedicine*, 2020, **15**(24), 2411–2427.

40 S. Y. Chang, K. Y. Huang, T. L. Chao, H. C. Kao, Y. H. Pang and L. Lu, *et al.* Nanoparticle composite TPNT1 is effective against SARS-CoV-2 and influenza viruses, *Sci. Rep.*, 2021, **11**(1), 1–13.

41 C. A. Devaux, J.-M. Rolain, P. Colson and D. Raoult, New insights on the antiviral effects of chloroquine against coronavirus: what to expect for COVID-19?, *Int. J. Antimicrob. Agents*, 2020, **55**(5), 105938.

42 S. Galdiero, A. Falanga, M. Vitiello, M. Cantisani, V. Marra and M. Galdiero, Silver Nanoparticles as Potential Antiviral Agents, *Molecules*, 2011, **16**(10), 8894–8918.

43 M. Rai, S. D. Deshmukh, A. P. Ingle, I. R. Gupta, M. Galdiero and S. Galdiero, Metal nanoparticles: The protective nanoshield against virus infection, *Crit. Rev. Microbiol.*, 2016, **42**(1), 46–56.

44 L. J. McGaw, E. E. Elgorashi and J. N. Eloff, *Cytotoxicity of African Medicinal Plants Against Normal Animal and Human Cells, Toxicol Surv African Med Plants*, 2014, pp. 181–233.

45 Washington DCS and RAD, *Reference Dose for Chronic Oral Exposure of Silver. CASRN 7440-22-4*, US Environ Prot Agency, 1991, pp. 1–13.

46 P. Examiner, *Ipnetrcsiatgye*, Azpuru CA, 2020, vol. 2.

47 S. D'Alessandro, M. Gelati, N. Basilico, E. A. Parati, R. K. Haynes and D. Taramelli, Differential effects on angiogenesis of two antimalarial compounds, dihydroartemisinin and artemisone: implications for embryotoxicity, *Toxicology*, 2007, **241**(1–2), 66–74.

48 Standard PCR Protocol.

49 C. Vonthron-Sénécheau, B. Weniger, M. Ouattara, F. T. Bi, A. Kamenan and A. Lobstein, *et al.* In vitro antiplasmodial activity and cytotoxicity of ethnobotanically selected Ivorian plants, *J. Ethnopharmacol.*, 2003, **87**(2–3), 221–225.

4304 | *Environ. Sci.: Nano*, 2022, **9**, 4295–4304

This journal is © The Royal Society of Chemistry 2022